

Light-Directed Electrical Stimulation of Neurons Cultured on Silicon Wafers

Artem Starovoytov, Jung Choi and H. Sebastian Seung

JN 93:1090-1098, 2005. First published Sep 22, 2004; doi:10.1152/jn.00836.2004

You might find this additional information useful...

Supplemental material for this article can be found at:

<http://jn.physiology.org/cgi/content/full/00836.2004/DC1>

This article cites 31 articles, 4 of which you can access free at:

<http://jn.physiology.org/cgi/content/full/93/2/1090#BIBL>

Updated information and services including high-resolution figures, can be found at:

<http://jn.physiology.org/cgi/content/full/93/2/1090>

Additional material and information about *Journal of Neurophysiology* can be found at:

<http://www.the-aps.org/publications/jn>

This information is current as of March 21, 2006 .

Light-Directed Electrical Stimulation of Neurons Cultured on Silicon Wafers

Artem Starovoytov, Jung Choi, and H. Sebastian Seung

Howard Hughes Medical Institute and Department of Brain and Cognitive Sciences, Massachusetts Institute of Technology, Cambridge, Massachusetts

Submitted 16 August 2004; accepted in final form 21 September 2004

Starovoytov Artem, Jung Choi, and H. Sebastian Seung. Light-directed electrical stimulation of neurons cultured on silicon wafers. *J Neurophysiol* 93: 1090–1098, 2005. First published September 22, 2004; doi:10.1152/jn.00836.2004. Dissociated neurons cultured in vitro can serve as a model system for studying the dynamics of neural networks. Such studies depend on techniques for stimulating patterns of neural activity. We show a technique for extracellular stimulation of dissociated neurons cultured on silicon wafers. When the silicon surface is reverse biased, electrical current can be generated near any neuron by pulsing a laser. Complex spatiotemporal stimulation patterns can be produced by directing a single beam with an acousto-optic deflector. The technique can generate a stimulating current at any location in the culture. This contrasts with multielectrode arrays (MEAs), which can stimulate only at fixed electrode locations. To characterize reliability and spatial selectivity of stimulation, we used intracellular (patch-clamp) recordings to monitor the effect of targeted laser pulses on cultured hippocampal neurons. Action potentials could be stimulated with submillisecond precision and 100-micron spatial resolution at rates exceeding 100 Hz. Optimal control parameters for stimulation are discussed.

INTRODUCTION

Cultured dissociated neurons are widely used for investigating the properties of synapses (Bi and Poo 1998; Goda and Stevens 1996) and molecules important in neural function (Sampo et al. 2003). They are also used to study the dynamics of neural networks (Bi and Poo 1999). For studying the behavior of networks, it is helpful to have ways of recording and stimulating activity patterns in many neurons simultaneously. For example, flat multielectrode arrays (MEAs) have become popular for this purpose (DeMarse et al. 2001; Gross 1979; Gross et al. 1993; Jimbo and Kawana 1992; Pine 1980; Shahaf and Marom 2001; Thomas et al. 1972). MEA approach, however, is hindered by a limited accuracy of individual addressing: randomly positioned cells don't usually match the predefined positions of microelectrodes. Controlled individual neuron-to-electrode interfacing in culture by means of growth guidance or immobilization has proven to be a challenging task (Fromherz et al. 1991; Maher et al. 1999; Sanjana and Fuller 2004; Zeck and Fromherz 2001).

Here we introduce a technique for electrical stimulation of neurons cultured on plain unprocessed silicon wafers. When a bias voltage is applied to the silicon/electrolyte interface, the silicon surface becomes depleted of majority carriers (Memming 2001). No current flows at the interface in the dark, but a local photocurrent can be generated with a laser pulse. Effectively, a "virtual" stimulating electrode is transiently created at a particular location on the silicon surface. The location of this virtual electrode is controlled by redirecting a

laser beam with an acousto-optic deflector, allowing the stimulation of spatiotemporal activity patterns.

Our approach is inspired by Colicos et al. (2001), who showed stimulation of neurons cultured on silicon by holding illumination constant and modulating bias voltage. Here we achieve true spatiotemporal control of stimulation by holding bias voltage constant and modulating illumination locally.

In contrast with MEA stimulation, possible stimulation sites are not limited to a set of fixed electrode locations. A "virtual" stimulation electrode can be transiently created at any location on the silicon. Our technique does not provide the recording capabilities of MEAs, but it could potentially be combined with optical imaging of neural activity for bi-directional communication with cultured networks.

Patch-clamp recordings of neurons were performed to monitor the effects of generating photocurrent at different locations. Some locations lead to direct stimulation of an action potential in the recorded neuron. Other locations lead to indirect stimulation, presumably due to synaptic input from other neurons that are directly stimulated. Spatial maps of these locations can be easily acquired by scanning the laser across the flat neural network. Our results suggest that distant processes are often more sensitive to stimulation than cell bodies, a view supported by some theoretical studies (McIntyre and Grill 1999; Rattay 1999) as well as by MEA experiments (Wagenaar et al. 2004).

The area of the network directly affected by our virtual electrode is roughly 100 microns in width. Possible reasons why this is broader than the illuminated spot are given in DISCUSSION. Temporal precision of stimulation is submillisecond, owing to the speed of the acousto-optic deflector. Repetitive stimulation of a neuron is possible at rates exceeding 100 Hz, essentially limited only by the refractory period of the neuron.

The generation of "virtual" electrodes on silicon exploits the properties of semiconductor electrode in contact with electrolyte. However, in its effects, our technique resembles other methods of electrically stimulating neurons. Therefore it enjoys the advantages that are typical of such methods, as well as the limitations. In particular, our technique is similar in its capabilities to MEA stimulation (Wagenaar et al. 2004). Comparison with other methods of optically controlled stimulation of neurons is found in DISCUSSION.

METHODS

Hippocampal cultures

Cells from P1–P2 rat hippocampi and culture media were prepared using a protocol described by Hagler and Goda (2001). The silicon base

Address for reprint requests and other correspondence: A. Starovoytov, 45 Carleton St., E25-425, Cambridge, MA 02139 (E-mail: artems@mit.edu).

of a specially designed culture dish (*Silicon culture plate fabrication*) was coated with poly-D-lysine/collagen. Cess (120,000–150,000) were plated onto each dish in 2 ml of culture medium. After 2 days, one-half of the medium was replaced with culture medium containing 8 μM ARA-C (cytosine arabinoside) to limit glia growth. Thereafter, the cells were fed weekly in the same manner with the medium containing 4 μM ARA-C.

Stimulation experiments were performed with 3- to 5-wk-old cultures. It should be emphasized that our cultures contained neurons growing on a monolayer of glial cells. After 3 wk in vitro, this layer was almost completely covering the silicon surface and could have some influence on electrical stimulation (see DISCUSSION).

Silicon culture plate fabrication

We used 375- μm -thick single-side-polished (100)-oriented silicon wafers boron-doped to 7–17 Ωcm (UniversityWafer.com and Virginia Semiconductor). Native oxide was left intact. Wafers with 100-nm thermal oxide layer and wafers with lower bulk resistivities were also tested. These produced inferior stimulation results (data not shown).

Holes of 1 cm diam were cut in the bottom of 35-mm culture dishes (Corning). The silicon wafers were cut into 1.5 \times 1.5-cm² square pieces and glued, polished side up, to the bottom side of each dish (Fig. 1, top). Silicone rubber was used for gluing (Dow Corning 3140). Prepared dishes were rinsed with ethanol before plating dissociated cells to improve wetting of the silicon surface.

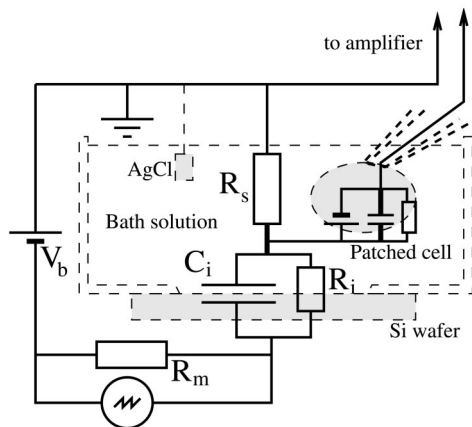
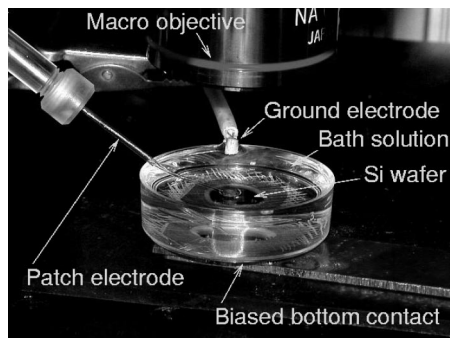


FIG. 1. Design of a culture dish used in electro-optical stimulation experiments. *Top*: image of the actual setup. Silicon wafer is glued to the bottom of the plastic culture dish. Neurons are plated onto the exposed silicon surface in the middle opening of the dish. Extracellular solution is grounded using Ag/AgCl electrode, and the bottom of the dish is contacted by a copper electrode with InGa eutectic painted onto the back side of silicon wafer. *Bottom*: equivalent circuit. C_i and R_i represent, correspondingly, the capacitance and the resistance of the double layer formed at the interface of electrolyte and semiconductor. V_b denotes the applied bias voltage; R_s is the resistance of electrolyte. Additional series resistor R_m was used for total current measurements. Extracellular potential for the patched cell is determined by the conditions immediately above the silicon surface.

Bias voltage

Our technique requires that a bias voltage be applied to the interface between the silicon and the solution above it. This was done by making ohmic electrical contact to the unpolished, back side of the wafer. The back side was scratched, painted with InGa eutectic (Aldrich Chemical Company), and placed on a flat copper electrode. The ground electrode was a silver/silver chloride pellet in the solution above the silicon. A DC power supply (Hewlett-Packard E3615A) was used to bias the back side negatively with respect to the ground electrode.

An equivalent circuit of this arrangement is shown in Fig. 1 (*bottom*). When a negative bias is applied to *p*-type silicon, it causes the silicon surface to be depleted of majority carriers. This depletion layer is important for our technique, because it allows silicon to be used as an electrode that is controlled by light. Both C_i and R_i dynamically depend on applied bias and illumination. In the dark, R_i is high, current is negligible, and the double layer capacitor C_i is charged by the applied voltage V_b . No measurable electric current was observed with moderately (~ 1 V) negative bias. When the silicon is illuminated, photogenerated electrons are driven to the surface (Zhang 2001). Depending on the applied bias, the result is either DC photocurrent or transient light-on and light-off currents (see discussion of Fig. 9).

When ionic current flows through the solution from the ground electrode toward the silicon substrate, the extracellular potential V_e near the silicon surface experiences an offset associated with ohmic resistance R_s (Fig. 1, *bottom*) of the bath solution. The resulting artifact is present in our captured patch voltage traces (RESULTS), providing a convenient marker for the temporal location of stimulating photocurrent pulse.

We used an additional 1-K Ω resistor in series with the sample (R_m in Fig. 1, *bottom*) to measure the stimulating current that was generated by pulsed illumination of the interface. Effects of applied bias, optical power, and pulse duration on the amplitude and shape of photocurrent pulses were studied. Results for bias dependence will be discussed in *Photocurrent dependence on stimulation parameters*. The same dishes with neural culture were used for photocurrent measurements to allow for possible modification of electro-chemical properties of semiconductor-to-solution interface due to the presence of biolayers. This technique measures the total photocurrent across the interface but does not reveal the detailed spatial profile of photocurrent density.

In principle, *n*-type silicon could be used instead of *p*-type silicon. The difference is that the back side would have to be biased positively relative to bath solution to produce a depletion layer. Under illumination, holes, rather than free electrons, would be pulled to the silicon/solution interface, which would lead to anodic oxidation of the silicon surface (Zhang 2001).

Targeted illumination pulses

The optical arrangement used in our experiments is shown in Fig. 2. A 660-nm laser diode (ML101J8, Mitsubishi) was powered by a Thorlabs LDC2000 controller. The illumination power measured at the sample ranged from 0.1 to 2 mW. A bi-axial acousto-optical deflector (AOD; 2DS-75-45-.633, Brimrose) was used for controlling beam position at the sample. The laser diode was coupled to the AOD through a 2-m-long optical fiber. The diffracted (1,1) component of AOD output, carrying roughly 50% of the optical power of the AOD input, was directed into a modified Olympus BXFM upright microscope and focused at the surface of the sample with a long working distance objective (XFluor 4x NA 0.28, 1-UB950). The low magnification objective provided a large field of view, exceeding 1 mm of the sample. The same objective was used to visualize the cultured neurons. Other components of the AOD output were stopped on apertures before the microscope. In addition, scan and tube lenses

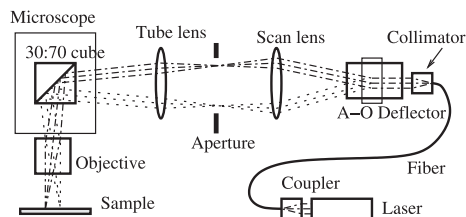


FIG. 2. Optical arrangement. Collimating and steering optics, the AOD, and the output coupler of the fiber were all rigidly attached to the microscope and moved together when translation across the sample was required. This allowed to keep the patch stationary at all times. The Tube and Scan lenses were introduced to lock the beam at the center of microscope objective for all deflection angles. Dash-dot and dotted lines show targeting different locations at the sample.

were used to guide the beam through the center of microscope objective for all the deflection angles (Tsai et al. 2002).

The *light-off* state was implemented with the AOD by directing the beam out of an aperture positioned in the focal plane between the scan and tube lenses. To produce a light pulse, the beam was directed to a target location for a desired duration, typically 100–200 μ s. AOD command voltages for *x* and *y* deflections of the laser beam were supplied by the two analog output channels of a National Instruments PCI-6052E acquisition board at 100 KHz. Since the access time of the AOD is roughly 10 μ s, it is possible to target several locations in the microscope field of view virtually simultaneously.

Electrophysiology and imaging

Whole cell patch-clamp recordings of neurons were performed in current-clamp mode (Axon Instruments Multi-Clamp 700A). The external bath solution had pH 7.3 and contained (in mM) 145 NaCl, 3 KCl, 10 HEPES, 3 CaCl₂, 8 glucose, and 2 MgCl₂ (Bi and Poo 1998). When only direct stimulation of the patched cell was of interest, synaptic transmission was blocked by adding the *N*-methyl-D-aspartate (NMDA) receptor antagonist D-2-amino-5-phosphonovalerate (D-AP5), the non-NMDA receptor antagonist 6-cyano-7-nitroquinoxaline-2,3-dione (CNQX), and the GABAergic chloride channel blocker picrotoxin (PTX) to bath solution in 100, 20, and 20 μ M concentrations, respectively. Partial replacement of the bath solution was performed every 1–2 h.

The internal solution of the electrodes (5–7 M Ω) contained (in mM) 130 K gluconate, 10 KCl, 5 MgCl₂, 0.6 EGTA, 5 HEPES, 0.06 CaCl₂, 2 Mg-ATP, 0.2 GTP, 0.2 leupeptine, and 20 phosphocreatine, and 50 U/ml creatine-phosphokinase (Arancio et al. 1995). At most, a 25 M Ω series resistance was considered acceptable in our recordings. Membrane resistances were typically 100–200 M Ω . All chemicals were purchased from Sigma-Aldrich.

To visualize neurites of patched cells, the fluorescent dyes Alexa Fluor 488 hydrozide or biocytin (A10436, A12924, Molecular Probes) were added to the pipette solution in a subset of our experiments. Concentrations of 5–10 mM were used. The dye was loaded by injecting negative current (2 nA) into the cell for 15 min following the laser-directed stimulation sessions, during which regions of successful stimulation of the patched cell were detected. Fluorescent images were acquired using Sensicam QE (Cook Corp.) and a Filter set (41012) from Chroma Technologies.

User interface and data presentation format

A graphical user interface was implemented in MATLAB. In one operating mode (point-and-shoot), a microscope image of the cultured neurons was displayed on the computer screen, and the user could click at any location in the image to send a laser pulse to that location. In the other mode (scan), the computer-directed laser pulses at a grid of points in a chosen rectangular area. The results of point-and-shoot experiments are displayed as individual intracellular recordings of

membrane voltage in response to laser stimulation. The results of scan experiments are displayed as two-dimensional (2D) maps of intracellular spike amplitudes or latencies with respect to stimulation location. A video of both types of data being acquired is available.¹

In scan mode without synaptic blockers (*Electrophysiology and imaging*), successive stimulations had to be separated by several hundred milliseconds. This allowed any network activity caused by the previous stimulation to die away before the next stimulation. With the sampled points separated by 50 μ m, the visible area of the sample was covered in \sim 5 min. With synaptic transmission blocked, samples were scanned in <1 min. The scans, as presented in the figures, were composed of top-to-bottom passes ordered from left to right.

RESULTS

Stimulation in the presence of synaptic transmission

An example of stimulation without synaptic blockers in the bath solution is shown in Fig. 3. Patch-clamp recordings of a single neuron were captured (Fig. 3B) while performing manual point-and-shoot stimulation of various locations (Fig. 3A, color markers). For each location, two to three traces of the same color are shown. During the first 10 ms after stimulation, the traces corresponding to same location superimpose almost perfectly, showing a high degree of reproducibility. The events around 20 ms after stimulation display some temporal jitter. The traces corresponding to different stimulation locations look quite different, showing that our technique has spatial specificity.

Complete visible area scans with grid spacing of 50 μ m were performed for the same patched cell. Figure 3C shows the peak voltage in response to stimulation. Some locations produce action potentials, while others produce subthreshold responses. The noisiness of the map is due to spontaneous activity. Figure 3D shows the timing of the peak voltage for suprathreshold events. Repeated scans of the sample produce roughly the same maps (data not shown).

Stimulation with synaptic transmission blocked

The dynamics of the intracellular voltage in Fig. 3 show a complex mixture of action potentials and subthreshold events. Some of this complexity could be due to synaptic inputs from other stimulated neurons. Therefore we performed experiments with synaptic blockers (AP5, CNQX, and PTX). A typical result is depicted in Fig. 4 (corresponding video record is available as supplemental material, see footnote 1).

Responses from the patched neuron (Fig. 4A) were recorded both in scan and in point-and-shoot modes. When the entire field of view was scanned, two areas of successful stimulation were detected (Fig. 4B, where the grayscale labeling of each tested location corresponds to the latencies relative to the stimulation pulse). This neuron was sensitive to stimulation in two regions, with, correspondingly, 8- and 11-ms delays. Stimulation near the soma had no effect. Notably, all the data points of the larger (the lower) area are characterized by the same latency, suggesting that the same “hot spot” in the culture was stimulated when pulsing the laser in this area.

Locations along the diagonal that crosses both hot spots were tested in point-and-shoot mode (Fig. 4, A and B, color-

¹ The Supplementary Material for this article (a video) is available online at <http://jn.physiol.org/cgi/content/full/00836.2004/DC1>.

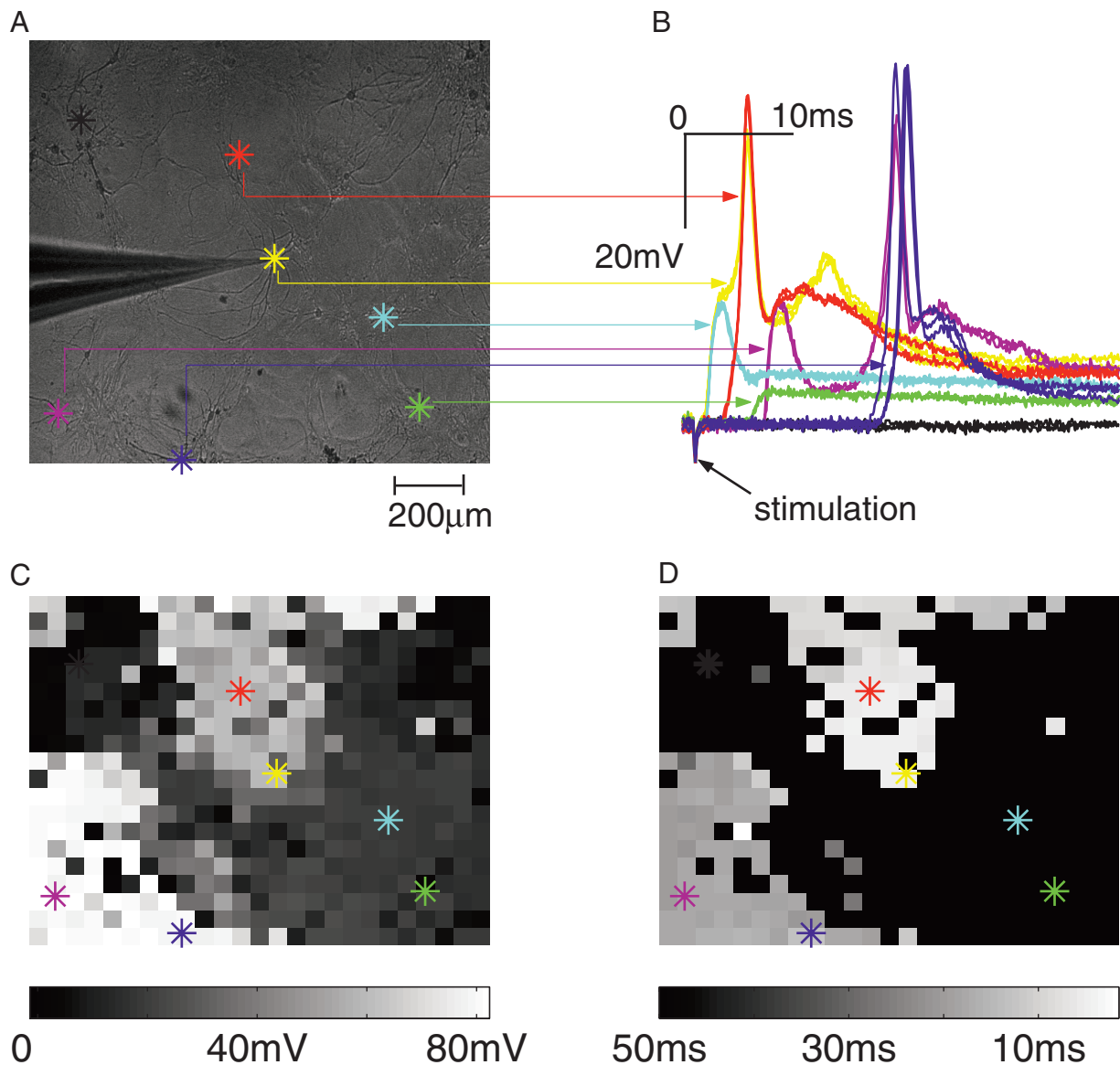


FIG. 3. Reproducible patterns of activity recorded from the patched neuron depending on optically addressed location. *A*: microscope image of neural network with color markers of selected targeted locations. *B*: individual traces of intracellular voltage recorded from the patched neuron following stimulation pulses. Colors refer to markers in *A*. Several traces shown for each location (each color) appear as one in most cases due to perfect reproducibility of neural response. Traces contaminated by spontaneous activity are not shown. *C*: 2D map of maximum amplitudes of intracellular voltage signals captured following stimulation pulses over 20×25 grid of target locations with $50\text{-}\mu\text{m}$ steps for the same patched cell as in *A* and *B*. Lighter shades of gray correspond to higher voltage amplitudes, see 0- to 80-mV grayscale bar at the bottom. *D*: temporal positions of peak voltage data-points relative to the time of stimulation, 0- to 50-ms grayscale bar at the bottom, events >50 ms after the pulse are not shown, and lighter color corresponds to earlier events. Fine-scale (single data points) noise in both *C* and *D* is due to spontaneous activity during the scan. Larger features of both amplitude and latency maps were reliably reproduced from scan to scan.

coded markers). Although voltage traces corresponding to 30 locations are shown in Fig. 4C, it is impossible to see them all in the graph. This is because the traces fall into three classes (2 distinctly different hot spots and all the other areas), and the traces within each class are almost identical, coinciding with an accuracy of $100\text{--}200\ \mu\text{s}$ (Fig. 4C, *inset*).

Because synaptic transmission has been eliminated, the results of stimulation are markedly different from Fig. 3. First, there are no subthreshold responses to stimulation. If the neuron responds at all, it generates an action potential. Second, the action potentials are stereotyped in shape; only the latency differs between stimulation sites. These properties were observed in all our experiments involving direct stimulation only,

that is, no synaptically mediated stimulation. Because of the stereotypy of the action potentials, it is likely that they are initiated in the axon, and travel antidromically to the soma, where they are recorded.

Latencies in the range of 1–20 ms were observed in our experiments. Similar surprisingly long (≤ 20 ms) latencies have been reported by other researchers when stimulating cultured neurons with multi-electrode arrays in the presence of synaptic blockers (Wagenaar et al. 2004).² It is not obvious

² Without synaptic blockers, stable responses with latencies even >20 ms have been observed (Bi and Poo 1999; Shahaf and Marom 2001).

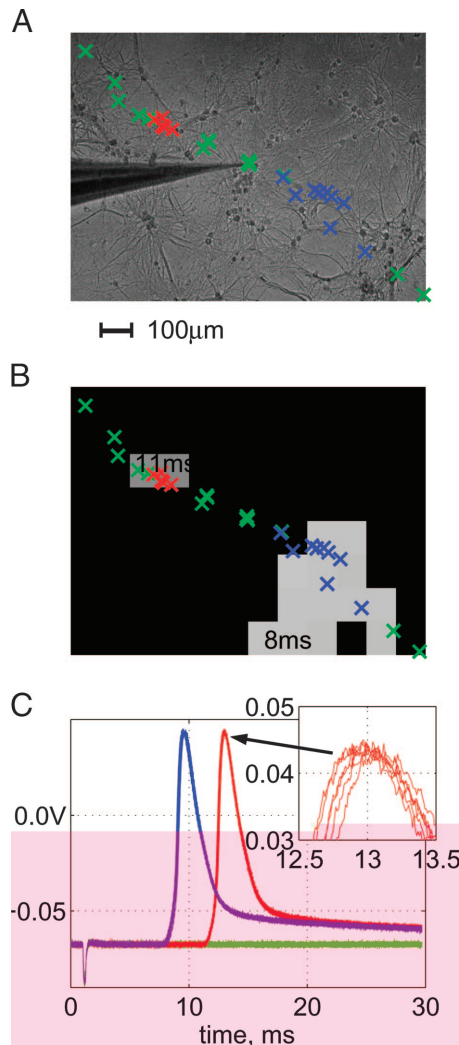


FIG. 4. Stimulation with synaptic connections blocked. *A*: microscope image of the neural network with locations of test pulses marked. *B*: spike-time-delay map acquired in scan mode with 100- μm step. Two separate “responding” areas are characterized by different delay values (shades of gray as marked). *C*: individual intracellular voltage traces acquired while pulsing the laser in locations marked in *A*.

how to explain these latencies, but they could arise if axons take long and tortuous paths in the culture.

The example shown in Fig. 4 is typical of all our experiments. In general, there were a few regions sensitive to stimulation for each patched cell. These regions might or might not include the soma. Our results suggest that fine processes like axons are more sensitive to electrical stimulation than somas, in agreement with the theoretical studies mentioned in the INTRODUCTION. Additionally, we find that the processes may contain a few sites that are especially sensitive, and these determine the sensitive regions of our technique. In some experiments, we recorded in succession from several neurons in one sample. For each neuron, a stimulation map was made. The maps for the different neurons had no relationship with each other (data not shown). This suggests that the maps reflect the morphology of individual neurons, a hypothesis that is tested in the following subsection.

Our technique allows repetitive stimulation of the same neuron with intervals as short as 10 ms. Stimulation by current

injection via patch electrode was characterized by roughly the same minimum interspike interval. This suggests that the temporal interval is limited by the refractory period of the neuron rather than by photo-electrochemical dynamics.

Fluorescent dye labeling of extended neurites

In 20 experiments, fluorescent dye was added to the pipette solution and loaded into the patched cell during the stimulation session. Images of labeled cells were captured after the patch electrode was removed. The locations of the hot spots, detected during the stimulation session, were matched to the visualized processes of the patched neuron. In five cases, a single neurite or a group of neurites crossed the areas of successful stimulation. An example is shown in Fig. 5. Synaptic transmission was blocked in this experiment, so no subthreshold events were observed (Fig. 5*B*). Three suprathreshold regions were detected by the scan with 2-, 4-, and 5-ms delays of the peak voltage relative to the stimulation pulse. One of the labeled neurites is passing the centers of all these three areas (Fig. 5, *B* and *C*). This neurite, which is fainter and longer than others and makes characteristic sharp turns, is believed to be an axon of the patched cell. The latencies of the three stimulated areas are consistent with the assumption that stimulation travels antidromically along this presumed axon. For example, the earliest response was observed when stimulating in the topmost region, which is much closer to the soma along the neurite compared with other two regions.

In 15 of 20 experiments, the detected hot spots did not match any of the labeled neurites. However, in these cases, there was no long thin neurite that looked like an axon. Therefore we believe that the negative results of these experiments were due to failure to successfully label axons. We do not believe that these experiments contradict the hypothesis of axonal stimulation.

Even if this hypothesis is accepted, it is still not clear why the axons were only susceptible to stimulation in a limited set of locations, rather than all along the visible paths. There must be other factors determining the locations of the observed hot spots. The primary candidates are spatial nonuniformities of silicon (native oxide) surface and discontinuities of glial layer growing on it (see DISCUSSION).

Optimal stimulation parameters

The amount of photocurrent produced by a laser pulse at the silicon depends on the value of the bias voltage, as well as on the intensity and duration of the illumination pulse. Therefore we studied the effects of varying these parameters on stimulation.

To characterize the spatial selectivity of stimulation, we measured the radius (or half-width) of the region where pulsing the laser was followed by action potential spikes in the patched neuron. When stimulation strength parameters were gradually adjusted from below to above the threshold of stimulation, neuronal responses would change from “no response” to probabilistic spikes in a narrow ($\leq 50 \mu\text{m}$) region to 100% reliable spikes in a $\geq 100\text{-}\mu\text{m}$ region with probabilistic spikes at the edges.

Figure 6*A* shows widening of the region sensitive to stimulation with the applied bias voltage. The summary is shown in Fig. 6*B*, where the analysis of linear 20- μm step scans across the responding area are presented. There is a threshold voltage above which

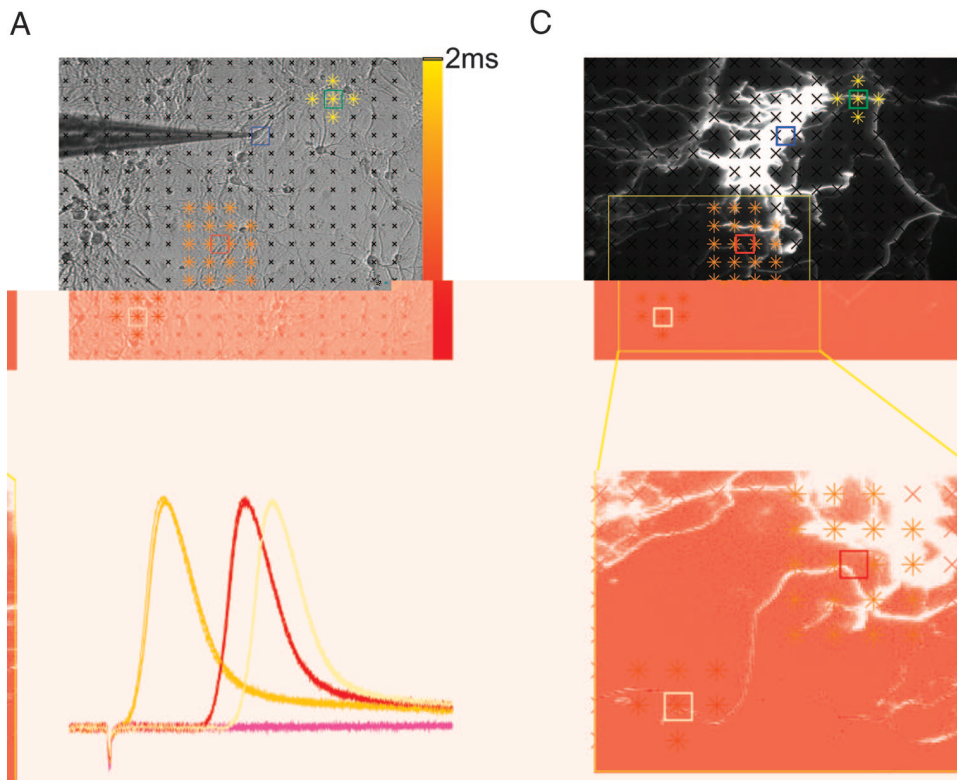


FIG. 5. Matching stimutable locations to visible neurites of the patched cell. *A*: bright-field image of the network with locations probed by a rectangular scan marked. Black “x” markers correspond to no response; color “*” markers correspond to action potential spikes of the patched cell with delays color-coded according to the color bar on the right. *B*: individual intracellular voltage traces following stimulation pulses in 4 different locations, see correspondingly colored square markers in *A*, *C*, and *D*. *C*: fluorescent image of the same cell acquired after the patched electrode was withdrawn. Tested locations are marked as in *A*. Image is overexposed to visualize the axon; hence the details of the complex dendrite morphology near the soma are not seen. *D*: zoomed-in and further overexposed region of the image in *C* as marked with a yellow rectangle, showing the axon crossing the centers of 2nd and 3rd regions of stimulation.

stimulation is possible. Above threshold, the width increases with increasing bias until saturation is reached.³

As discussed below, these graphs also depend on the illumination. Data acquired from different experiments are shown in the same plot to show the dependence on illumination power and duration as well as variations between different neurons. The saturated value for stimulation range could be kept below a radius of 100 μm by adjusting illumination parameters.

The dependence of stimulation range on illumination parameters is shown in Fig. 7. In Fig. 7*A*, illumination power is varied, while bias voltage and illumination duration are held constant. In Fig. 7*B*, illumination duration is varied, while bias voltage and illumination power are held constant. Again, the graphs have a threshold and a saturation.

Based on our results from many experiments, illumination at 0.3 mW for 100 μs was typically optimal for all tested cells. Threshold bias values for different neurons, on the contrary, were found to vary in a wide range (-0.4 to 1.5 V) from neuron to neuron. Furthermore, different *responding* locations for the same cell were usually found to “turn on” at different bias values. This is shown in Fig. 8, where spike-time-delay data recorded from the same cell are shown for different bias values applied during the scans. New *responding* locations were “turned on” when bias was increased from 0.4 to 0.45 and to 0.50 V. Further increase in bias value caused the *responding* areas to broaden, which corresponds to a loss of spatial selectivity: all three regions are seen merging at 0.65 V (*bottom right subplot*). Note that at 0.4 V bias (*top left subplot*), only a 4-ms delayed spike stimulated in a remote low-threshold

(*rightmost*) location was detected, while the nearest, possibly somatic, stimulation did not reach the threshold (see the brightest area in all the other subplots characterized by 2-ms delay).

Reliability of stimulation

More than 100 silicon culture dish samples were used in our experiments, with 3–10 cells patched on each sample. Because the goal of this study was to investigate the direct stimulation capabilities of the technique, synaptic connections were blocked most of the time. For approximately two of three patched cells, it was possible to achieve stimulation within the available range of stimulation strength, in which cases one to four different stimulation sites were typically detected for each cell with variable spatial precision depending on the stimulation strength used. Both the reliability and the selectivity of stimulation are thus dependent on the stimulation parameters. According to our statistics, maximizing the strength of the photocurrent pulse allows stimulation of roughly 70% of cells in culture while setting the stimulation strength parameters to lower values provides for more selective addressing of a lower percentage of cells. For example, when using -0.6 V bias with 100- μs pulses of 0.3-mW illumination in the presence of synaptic blockers, stimulation sites were observed for only about 20% of the patched cells.

Without synaptic blockers, reproducible intracellular voltage changes following stimulation pulses were detected in 100% of patched cells.

Photocurrent dependence on stimulation parameters

To address the physical nature of this wide variation of threshold bias values and to show the extracellular currents associated with pulsed illumination of the substrate in our

³ The curves in Figs. 6*B* and 7 should not be taken literally: half-width values approaching zero near and below thresholds correspond to unreliable stimulation in a narrow subset of locations probed by the scan and do not in fact mean an improved resolution for subthreshold stimulation strength.

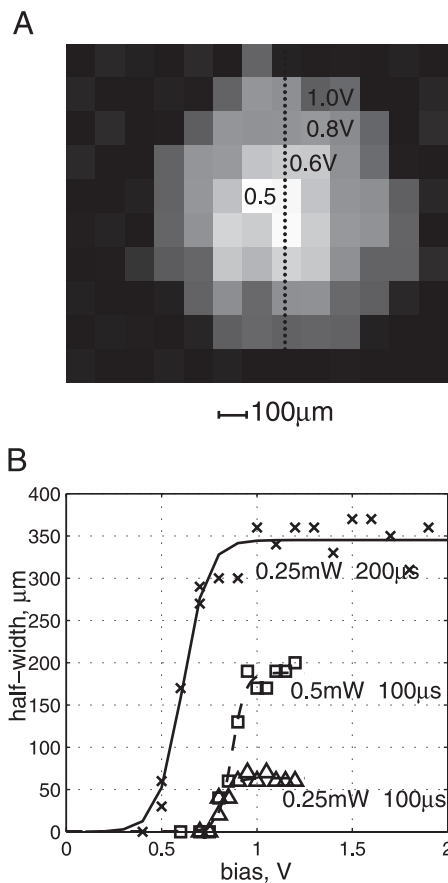


FIG. 6. Widening of stimulation range with applied bias increase. *A*: maps of locations where light pulses were followed by spikes in the patched neuron. Results for different applied bias values are plotted on top of each other; 100- μm scan step was used in each case. Different shades of gray correspond to bias values -0.5 , -0.6 , -0.8 , and -1.0 V, counting from the center. *B*: “ \times ” markers and solid line: summary of width vs. bias dependence measured by means of a linear 20- μm step scan across the *responding* area (see dots in *A*) performed at various bias values, fitted with a sigmoid function. Square and triangle markers and dashed lines: data acquired from a different patch. Illumination parameters are shown near each graph.

culture dishes, the dependence of photocurrent amplitude and shape on the applied bias is shown in Fig. 9. Two illumination pulses, 0.3- and 10-ms duration, of 0.5-mW optical power focused into 10 μm FWHM (full-width-at-half-maximum) spot were used for all tested bias values. The following properties of the silicon-to-solution interface were observed: 1)

measurable photocurrent was only present at bias values below negative 0.4–0.5 V; 2) photocurrent amplitude saturated at around -1.4 V (see the emphasized light gray curve), with further increase of applied bias affecting only the shape of photocurrent pulses; and 3) the *weak* bias regimen was characterized by purely capacitive biphasic photocurrent (see the emphasized black curve corresponding to -0.6 V bias), DC photocurrent was observed in the *strong* bias regimen (the last curve corresponds to -1.9 V), and slower transient features were present in the *intermediate* bias range (see the emphasized dark gray curve corresponding to -0.9 V).

Increasing illumination pulse duration in the *weak* bias regimen had no effect on the photocurrent amplitude and only a limited effect on total charge transferred (data not shown). Increasing optical power in the *weak* bias regimen had a limited effect on photocurrent amplitude and almost no effect on the amount of charge transferred (data not shown).

DISCUSSION

We have shown a method for extracellular electrical stimulation of neurons. Our method is applicable to neurons cultured on silicon, which serves simultaneously as substrate and stimulating electrode. When an appropriate bias voltage is applied, only the illuminated region of the silicon passes current, so that the stimulating electrode is light-addressable.

Multielectrode arrays can also be used for spatially controlled electrical stimulation, but only at the fixed locations on the array. With our method, any location is addressable through control of the illumination. Furthermore, our method has the advantage of using low-cost, disposable substrates.

Other methods for using light to control stimulation of neurons have been proposed. For example, a laser can be used to uncage the excitatory neurotransmitter glutamate, which stimulates neurons through glutamate receptors (Katz and Dalva 1994; Shepherd et al. 2003). Chemical stimulation has the virtue that it does not stimulate axons, unlike electrical stimulation. However, it has less temporal precision and may not be useful for repetitive stimulation if receptors desensitize. Another method is to express light-sensitive ion channels in neurons and stimulate with light (Zelman et al. 2002). For this method, the latency to stimulation ranges from several hundred milliseconds to several tens of seconds, so the temporal control is not very fine, although the spatial resolution is very good.

To characterize our stimulation technique, we have combined it with intracellular recordings of neurons. To our knowl-

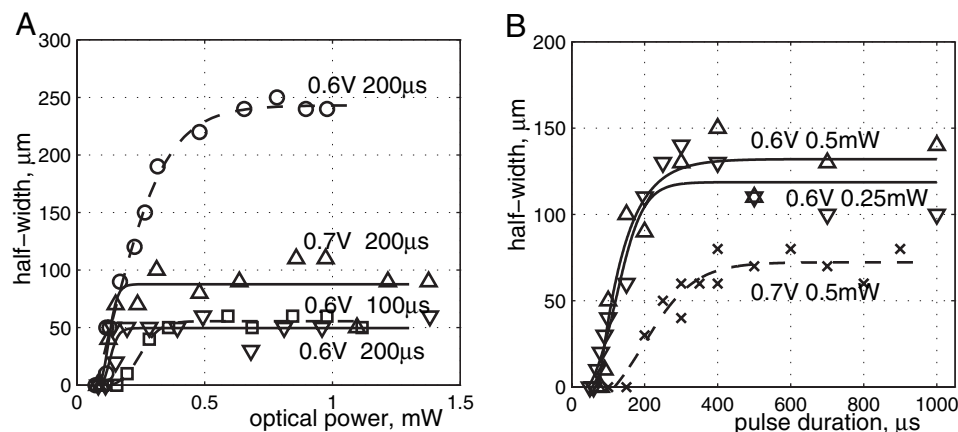


FIG. 7. Stimulation range dependence on (*A*) optical power and (*B*) duration of the illumination pulse. Data acquired by means of linear scans (10- or 20- μm steps) as explained in caption for Fig. 6. Triangle markers and solid lines in both *A* and *B* correspond to data acquired from the same patched cell. Compare with data from other cells, dashed lines.

[REDACTED]

method to be useful for creating spatiotemporal patterns of activity in neurons, as shown in Fig. 3.

Excluding the added radius due to passing fibers, the spatial resolution intrinsic to our technique is around 100 microns, which is in agreement with the expected bulk diffusion length assuming a sub-10- μ s minority carrier lifetime (Bousse et al. 1994). One can imagine some possible ways of improving this. One possibility is to dope the silicon with gold. The recombination centers should reduce the lateral diffusion of photogenerated minority carriers. Another possibility is to platinize the silicon surface to facilitate charge transfer from the silicon to the solution (Dominey et al. 1982). One can also imagine methods of patterning the silicon surface to improve the spatial resolution.

The structure and the operating principles of our stimulating electrode resemble those of a light-addressable potentiometric sensor (LAPS), except that no oxide layer is intentionally grown on the semiconductor surface. The LAPS is a semiconductor-insulator-electrolyte device for measurement of local surface potential changes, with the measurement point conveniently controlled by scanning the laser (Ismail et al. 2002; Parak et al. 1997). As in the case of LAPS, we locally modulate conductivity in the depletion layer of semiconductor by means of local free carrier photogeneration. Minority carrier diffusion is believed to put a limitation on the spatial resolution of LAPS (George et al. 2000), which supports our understanding of the observed stimulation range broadening. Interestingly, the use of LAPS for extracellular recording of spiking activity in plated cells is being investigated (Ismail et al. 2003). It is too early to know whether integrating such recording with our stimulation technique is feasible because extracellular voltage changes to be recorded are near detection threshold for LAPS and optimizing the device for recording may contradict the optimal stimulation recipe laid out in this article.

ACKNOWLEDGMENTS

We thank D. Hafeman and S. Manalis for advice about the silicon-electrolyte interface, D. Kleinfeld and C. Fang-Yen for help with optics, and N. Agnihotri for stimulating discussions. We are also grateful to Y. Goda for providing information about cell culture methods, as well as the stimulation technique of Colicos et al. 2001. B. Li and G. Liu generously taught us cell culture techniques.

GRANTS

This research is sponsored by the Howard Hughes Medical Institute.

REFERENCES

- Arancio O, Kandel E, and Hawkins R.** Activity-dependent long-term enhancement of transmitter release by presynaptic 3',5'-cyclicGMP in cultured hippocampal neurons. *Nature Lett* 376: 74–80, 1995.
- Bard AJ and Faulkner LR.** *Electrochemical Methods*. New York: John Wiley, 2001.
- Bi G and Poo M.** Distributed synaptic modification in neural networks induced by patterned stimulation. *Nature* 401: 792–796, 1999.
- Bi GG and Poo MM.** Synaptic modifications in cultured hippocampal neurons: dependence on spike timing, synaptic strength, and postsynaptic cell type. *J Neurosci* 18: 10464–10472, 1998.
- Bousse L, Mostarshed S, Hafeman D, Sartore M, Adami M, and Nicolini C.** Investigation of carrier transport through silicon wafers by photocurrent measurements. *J Appl Physiol* 75: 4000–4008, 1994.
- Colicos MA, Collins BE, Sailor MJ, and Goda Y.** Remodeling of synaptic actin induced by photoconductive stimulation. *Cell* 107: 605–616, 2001.
- DeMarse N, Wagenaar D, Blau A, and Potter S.** The neurally controlled animat: biological brains acting with simulated bodies. *Autonomous Robots* 11: 305–310, 2001.
- Dominey R, Lewis N, Bruce J, Bookbinder D, and Wrighton M.** Improvement of photoelectrochemical hydrogen generation by surface modification of p-type silicon semiconductor photocathods. *J Am Chem Soc* 104: 2412, 1982.
- Fromherz P, Schaden H, and Vetter T.** Guided outgrowth of leech neurons in culture. *Neurosci Lett* 129: 77–80, 1991.
- Fromherz P and Stett A.** Silicon-neuron junction: capacitive stimulation of an individual neuron on a silicon chip. *Phys Rev Lett* 75: 1670–1673, 1995.
- George M, WJ P, Gerhardt I, Moritz W, Kaesen R, Geiger H, Eisele I, and Gaub H.** Investigation of the spatial resolution of the light-addressable potentiometric sensor. *Sensors Actuators* 86: 187–196, 2000.
- Goda Y and Stevens CF.** Long-term depression properties in a simple system. *Neuron* 16: 103–111, 1996.
- Gross G.** Simultaneous single unit recording in vitro with a photoetched laser deinsulated gold multielectrode surface. *IEEE Trans Biomed Eng* 26: 273–279, 1979.
- Gross G, Rhoades B, Reust D, and Schwalm F.** Stimulation of monolayer networks in culture through thin-film indium-tin oxide recording electrodes. *J Neurosci Methods* 50: 131–143, 1993.
- Hagler DJJ and Goda Y.** Properties of synchronous and asynchronous release during pulse train depression in cultured hippocampal neurons. *J Neurophysiol* 85: 2324–2334, 2001.
- Ismail A, Furuichi K, Yoshinobu T, and Iwasaki H.** Light-addressable potentiometric fluoride sensor. *Sensors Actuators* B86: 94–97, 2002.
- Ismail A, Yoshinobu T, Iwasaki H, Sugihara H, Yukimasa T, Hirata I, and Iwata H.** Investigation on light-addressable potentiometric sensor as a possible cellsemiconductor hybrid. *Biosens Bioelectron* 18: 1509–1514, 2003.
- Jimbo Y and Kawana A.** Electrical stimulation and recording from cultured neurons using a planar electrode array. *Bioelectrochem Bioenerget* 29: 193–204, 1992.
- Katz L and Dalva M.** Scanning laser photostimulation: a new approach for analyzing brain circuits. *J Neurosci Methods* 54: 205–218, 1994.
- Maher M, Pine J, Wright J, and Tai Y.** The neurochip: a new multielectrode device for stimulating and recording from cultured neurons. *J Neurosci Methods* 87: 45–56, 1999.
- McIntyre C and Grill W.** Excitation of central nervous system neurons by nonuniform electric fields. *Biophysics J* 29: 878–888, 1999.
- Memming R.** *Semiconductor Electrochemistry*. Weinheim, Germany: Wiley-VCH, 2001.
- Parak W, Hofmann U, Gaub H, and Owicki J.** Lateral resolution of light-addressable potentiometric sensors: an experimental and theoretical investigations. *Sensors Actuators* A63: 47–57, 1997.
- Pine J.** Recording action potentials from cultured neurons with extracellular microcircuit electrodes. *J Neurosci Methods* 2: 19–31, 1980.
- Rattay F.** The basic mechanism for the electrical stimulation of the nervous system. *Neuroscience* 89: 335–346, 1999.
- Sampo B, Kaech S, Kunz S, and Banker G.** Two distinct mechanisms target membrane proteins to the axonal surface. *Neuron* 37: 611–624, 2003.
- Sanjana N and Fuller S.** A fast flexible ink-jet printing method for patterning dissociated neurons in culture. *J Neurosci Methods* 136: 151–163, 2004.
- Shahaf G and Marom S.** Learning in networks of cortical neurons. *J Neurosci* 21: 8782–8788, 2001.
- Shepherd G, Pologruto T, and Svoboda K.** Circuit analysis of experience-dependent plasticity in the developing rat barrel cortex. *Neuron* 38: 277–289, 2003.
- Thomas C, Springer P, Loeb G, Berwald-Netter Y, and Okun L.** A miniature microelectrode array to monitor the bioelectric activity of cultured cells. *Exp Cell Res* 74: 61–66, 1972.
- Tsai PS, Nishimura N, Yoder EJ, Dolnick EM, White GA, and Kleinfeld D.** Principles, design, and construction of a two-photon laser scanning microscope for in vitro and in vivo brain imaging. In: *In Vivo Optical Imaging of Brain Function*, edited by Frostig RD. Boca Raton, FL: CRC Press, 2002, p. 113–171.
- Wagenaar DA, Pine J, and Potter SM.** Effective parameters for stimulation of dissociated cultures using multi-electrode arrays. *J Neurosci Methods* 138: 27–37, 2004.
- Zeck G and Fromherz P.** Noninvasive neuroelectronic interfacing with synaptically connected snail neurons immobilized on a semiconductor chip. *Proc Nat Acad Sci USA* 98: 10457–10462, 2001.
- Zemelman B, Lee G, Ng M, and Miesenbock G.** Selective photostimulation of genetically chARGed neurons. *Neuron* 33: 15–22, 2002.
- Zhang XG.** *Electrochemistry of Silicon and Its Oxide*. New York, NY: Klumer Academic/Plenum Publishers, 2001.